OXFORD

SOT | Society of Toxicology
www.toxsci.oxfordjournals.org

TOXICOLOGICAL SCIENCES, 143(2), 2015, 441–453

doi: 10.1093/toxsci/kfu243
Advance Access Publication Date: December 1, 2014

Glucocorticoids Exert Direct Toxicity on Microvasculature: Analysis of Cell Death Mechanisms

Ikram El Zaoui[*,†,‡], Francine Behar-Cohen[*,†,‡,§,1], and Alicia Torriglia[*,†,‡,1,2]

[*]INSERM UMRS 1138, Team 17 from Physiopathology of Ocular Diseases to Clinical Developments, Paris, France, [†]Pierre et Marie Curie University, [‡]Paris Descartes University, UMRS 1138, Centre de Recherche des Cordeliers 75006, Paris, France and [§]Hopital Ophtalmique Jules Gonin 1000, Lausanne, Switzerland

[1]These authors contributed equally to this study.
[2]To whom correspondence should be addressed at INSERM UMRS 1138, Centre de Recherches des Cordeliers, Team 17 from Physiopathology of Ocular Diseases to Clinical Developments; Pierre et Marie Curie University; and Descartes University, 15 rue de l'école de médecine, F-75006 Paris, France. Fax: +33 1 44 27 81 83. E-mail: alicia.torriglia@inserm.fr.

ABSTRACT

Glucocorticoids (GCs) are routinely administered systemically or injected into the eye when treating numerous ocular diseases; however, their toxicity on the retinal microvasculature has not been previously investigated. In this article, the effects of hydrocortisone (Hydro), dexamethasone, dexamethasone-phosphate and triamcinolone acetonide (TA) were evaluated *in vitro* on human skin microcirculation cells and, bovine endothelial retinal cells, *ex-vivo*, on flat mounted rat retinas. The degree of GCs induced endothelial cell death varied according to the endothelial cell type and GCs chemical properties. GCs toxicity was higher in skin microvascular endothelial cells and for hydrophobic GC formulations. The mechanism of cell death differed between GCs, Hydro and TA activated the leukocyte elastase inhibitor/L-DNase II pathways but did not activate caspases. The mechanisms of cell death observed in cell cultures were similar to those observed in rat retinal explants. Taken together these results indicate that particular attention should be paid to the potential vascular side effects when administrating GCs clinically and in particular when developing sustained-release intraocular devices.

Key words: glucocorticoids; endothelial cell; retinal microvasculature; apoptosis; dermic endothelial cell

Glucocorticoids (GCs) hormones easily cross cell membranes due to their lipophilicity and exert physiological effects in almost every tissue of the human body (Cockrem, 2013; Walker *et al.*, 2012). Synthetic or semi-synthetic GCs aim to optimize the immunosuppressive, angiostatic, and anti-inflammatory properties of cortisol, while reducing their mineralocorticoid side effects. GCs remain the first-line therapy in number of inflammatory conditions and are administered locally or systemically (Barnes, 2005; Logie *et al.*, 2010). Recognized side effects of GCs include microvascular fragility, atrophy, as well as reduced microvascular density in skin, bone, and muscle (Anacker *et al.* 2011; Schacke *et al.* 2002; Torriglia *et al.*, 2010).

Folkman *et al.* demonstrated that hydrocortisone (Hydro) and dexamethasone (Dexa) at micrograms per microliters concentrations prevent heparin-stimulated angiogenesis in the chick chorioallantoic membrane and induce the regression of capillaries within the surrounding tissue (Folkman *et al.*, 1983; Folkman and Ingber, 1987). Later, Small *et al.* showed that corticosterone (300–600 nM) inhibits angiogenesis *in vitro* and *in vivo*. In addition, inhibition of 11-beta-hydroxysteroid dehydrogenase type 1 favors corticosterone production and enhances angiogenesis providing evidence for the angiostatic role of endogenous corticosteroids (Small *et al.*, 2005). More recently, the mechanisms of the angiostatic effects of physiological doses of the endogenous corticosterone have been studied in more details, revealing a receptor-mediated effect on vascular endothelial growth factor production, activation of matrix metallo peptidase 2, and the inhibition of endothelial cells tube-like structure formation (Shikatani *et al.*, 2012). Systemic administration of GCs triggered cell death of macrophages (Schmidt

et al., 1999), human epithelial cells of the lens (Sharma *et al.*, 2011), pericytes (Katychev *et al.*, 2003), and induced necrosis of microvessels and osteocytes in the co-femoral articulation and bruises (Allen *et al.*, 2003; Hu *et al.*, 2006).

The possibility that higher doses of corticosteroids may exert further direct effects on an established microvasculature has not been extensively explored.

In ophthalmology clinics, GCs are commonly used to treat ocular inflammation as well as macular edema of inflammatory and non-inflammatory origins such as diabetic retinopathy or retinal vein occlusion. As chronic use is often required, high doses of the hydrophobic triamcinolone acetonide (TA) or polymeric implants releasing Dexa for sustained periods are used to reduce the frequency of intraocular administrations (Behar-Cohen, 2011). In addition, ocular tissues are resistant to the use of GCs due to the high concentration of endogenous steroid (Knisely *et al.*, 1994), explaining the high concentrations (about 1 mg/ml) used clinically. GCs exert rapid and striking effects on retinal edema (Miyamoto *et al.*, 2006) but are associated with potential side effects on the posterior segment of the eye including a reduction of the choroidal vascular network, decreased retinal vessel diameter in rats, and a decrease in the retinal vascular density in the developing retinal vasculature (Hartnett *et al.*, 2006; Valamanesh *et al.*, 2009). Whether GCs directly affect endothelial cell viability has not been fully explored.

On the one hand, when compared with bone, muscle, or skin where the vasculature undergoes constant remodeling, retinal endothelial cells proliferate at a very slow rate under normal conditions (Joussen *et al.*, 2007). On the other hand, GCs have failed to demonstrate anti-angiogenic effects on retinal or choroidal neovascularization (Chan *et al.*, 2011; Geltzer *et al.*, 2013) suggesting that GCs may exert different effects on endothelial cells derived from different tissue origin. We have previously shown that clinical doses of intraocular TA induced a caspases-independent apoptosis associated with the absence of TUNEL labeling on bovine retinal endothelial cells in culture and in retinal neovessels (Torriglia *et al.*, 2010; Valamanesh *et al.*, 2009). This suggested that non-classical mechanisms of cell death such as autophagy, caspases-independent apoptosis, or necrosis (Galluzzi *et al.*, 2012) could be involved in GCs toxicity.

Taken together, these results suggest that the molecular mechanisms underlying GCs effects on the vasculature are complex and involve different cellular and molecular pathways depending on the endothelial cell type, the GC concentration, and duration of exposure.

The aim of this study was to compare the potential toxicity of commonly used GCs (Le Jeunne, 2012) on vascular endothelial cells of different origin and to investigate the underlying mechanisms of toxicity of the different GCs. This is particularly important given that the evaluation of toxicity relies frequently on caspases-dependent markers and could be underestimated if other molecular mechanisms are involved. The relevance of our *in vitro* findings was assessed by analyzing GCs effects on rat retinal explants.

MATERIALS AND METHODS

Animals. Adult male Lewis rats (6–8 weeks old; Janvier, Le Genest-Saint-Isle, France) were used for the *ex-vivo* experiments. Rats were sacrificed using carbon dioxide inhalation. All experiments were performed in accordance with the European Communities Council Directive 86/609/EEC and approved by the local ethical committee of University Paris Descartes.

Human dermal microvascular endothelial cell culture. All culture media and additives were purchased from Invitrogen (Cergy Pontoise, France). GCs were purchased from Sigma-Aldrich (Saint-Quentin Fallavier, France).

Human dermal microvascular endothelial cells (HMECs) are a transformed cell line transfected with a PBR-322 plasmid containing a region encoding for the SV40 (Simian Virus) gene (Ades *et al.*, 1992). Cultures were maintained at 37°C in a humidified atmosphere containing 5% CO_2. They were cultured in the endothelial basal medium supplemented with L-glutamine and HEPES 15mM, 10% complement-free fetal calf serum (DFCS), and 1% streptomycin (100 µg/ml)—penicillin (100 units/ml). Confluent HMECs were treated with the LC_{50} of GCs: 275 µM Hydro, 255 µM Dexa, 230 µM TA, and 2 mM dexamethasone-phosphate (Dexa-Ph) in media supplemented with 2% of DFCS for 24 h. Although cell survival reaches a plateau with Dexa-Ph, 2 mM was the concentration giving the most reproducible results. The hydrophobic GCs (all except for Dexa-Ph) were previously dissolved in ethanol 100% and then in the medium (ethanol final concentration 1%). This last step was introduced in order to have a known concentration of the GCs in the treatment media. Actually, without this step, hydrophobic GCs such as TA, for instance, precipitate in aqueous medium. This alters the real concentration of the GC and generates crystals that precipitate, stick to cells, and cause mechanical damage.

Bovine retinal endothelial cell culture. Bovine retinal endothelial cells (BRECs) were isolated from the bovine retinal microcirculation as previously reported (Capetandes and Gerritsen, 1990). BRECs were grown in Dulbecco's Modified Eagle's Medium (DMEM) supplemented with GlutaMAX, 4.5 g/l glucose, 10% decomplemented fetal calf serum (DFCS), 1% streptomycin (100 µg/ml)—penicillin (100 units/ml), 0.5% fungizone-amphotericine, and 20 ng/ml basic Fibroblast Growth Factor (FGFb). Cultures were maintained at 37°C in a humidified atmosphere containing 5% CO_2. Confluent BRECs were treated with LC_{50} GCs 1.37 mM for Hydro, 765 µM Dexa, 460 µM TA, and 2 mM for Dexa-Ph in media supplemented with 2% DFCS for 24 h. The hydrophobic GCs (all except Dexa-Ph) were previously dissolved in ethanol 100% then in the medium (ethanol final concentration 1%). This cell line was chosen due to the difficulties of obtaining an equivalent from human origin.

Rat retinal explants. After enucleation, rat retinas were isolated immediately under aseptic conditions. They were flattened by 4 orthogonal incisions, then transferred onto a Cyclopore 0.2 µm polycarbonate membrane (Whatman, Maidstone, UK), and mounted with the vitreal side up. The support membranes were placed in 6-well tissue culture plates containing 2 ml DMEM supplemented with 10% steroid-free FCS, 1% penicillin-streptomycin, and 0.1% amphotericin-B. Explants were treated with LC_{50} of BRECs as described for cultured BRECs.

MTT Assay. The MTT assay is a colorimetric test that was developed to determine the survival and growth of eucaryotic cells in proliferation or to evaluate cytotoxicity (Mosmann, 1983). The ability to reduce the tetrazolium salts by HMEC and BRECs was used to evaluate the toxicity and LC_{50} of GCs. Briefly, cells were seeded in a 24-multi-well plates at a density of 5×10^4 cells in 1 ml of complete medium. Confluent cells were treated during 24 h with increasing concentrations of CGs. At the end of the

treatment, 250 µl of CellTiter 96 Non-Radioactive Cell Proliferation Assay (MTT; Promega, G4000) (5 mg of MTT per ml of phosphate-buffered saline) was added to each well, including 6 wells that contained only medium or medium containing 1% ethanol (controls). Plates were then incubated for 1 h at 37°C in the dark and analyzed with a microplate reader (BioRad Benchmark, Paris, France) at 570 versus 630 nm. Experiments were performed in triplicate and repeated 3 times.

Caspases Inhibition

Thirty minutes prior to treatment, HMECs were incubated in 10 µM benzoyloxycarbonyl-val-ala-asp-fluoromethyl ketone (ZVAD-FMK) (ApexBio A1902). Treatment was initiated by adding GCs at the LC_{50} concentrations in the same medium. Controls included 0.2% Dimethyl sulfoxide (DMSO), the vehicle of ZVAD (not shown). Etoposide treatment, 100 µM for 24 h, was used as a positive control of caspases activation. Cell survival was measured by the MMT method.

Internucleosomal DNA Degradation

Internucleosomal DNA degradation assay was performed as described by Zhua *et al.* (Ning Zhua 1997). Briefly, cells from each condition were obtained by scraping in culture medium. A cell pellet was obtained by centrifugation at 173 g for 10 min, then the pellet was extracted in 30 µl of sarkozyl (50mM of Tris, 10mM of EDTA, 2% of N-lauryl sarcosine at pH 7.5) and immediately stored on ice. The cellular lysates were then treated for 2 h with 1 µl of proteinase K 20 mg/ml at 45°C, and 1 µl of RNase-A 10 mg/ml for 1 h at 37°C. Finally, the DNA samples were run in a Tris-acetate-EDTA 2% agarose gel and visualized by staining with ethidium bromide.

Lactate Dehydrogenase Assay

Lactate dehydrogenase (LDH) is a cytoplasmic enzyme not released during active cell death like apoptosis, paraptosis, or autophagy, but released in necrosis due to the early increase of plasma membrane permeabilization. The LDH assay was performed according to the manufacturer's instructions of the LDH Cytotoxicity Detection Kit (Roche Applied Sciences). Following GCs treatment, an aliquot of culture supernatant was immediately stored on ice. Cells incubated with 1% Triton-X100 represented the positive control (100% of LDH release). The enzymatic reaction was initiated by the addition of 100 µl of reaction mixture (provided in the kit) with 100 µl of supernatant during 30 min at room temperature. Reaction products were assessed spectrometrically at an absorbance of 490 versus 630 nm in 96 multi-well plates. The percentage of lysed cells was calculated using the following formula: 100 × [(experimental LDH release)/(maximum LDH release)]. The maximum of LDH release corresponding to the amount of LDH released by a total lysis of the cells with Triton-X100. These experiments were performed 4 times.

Indirect Immunofluorescence Experiments

Cells were seeded at density of 5×10^4 cells in 1 ml of complete medium in Lab-Tek devices (4 wells, Glass slide). Confluent cells were treated with LC_{50} of GCs at the indicated concentrations according to the cellular origin. The following proteins were tested: Light Chain 3 (LC3), cleaved Caspase-3, apoptosis inducing factor (AIF), and leukocyte elastase inhibitor (LEI)-derived DNase II (LEI/L-DNase II). At the end of the treatments, cells were washed 3 times with phosphate buffer saline (PBS), fixed with 4% paraformaldehyde for 15 min at room temperature, washed 3 times in PBS, permeabilized with 0.3% de Triton-X100 for 15 min, washed 3 times with PBS for 5 min, and then saturated with 1% bovine serum albumin (BSA) in PBS for 1 h. Slides were then incubated with the polyclonal antibody against LC3 (Santa Cruz Biotechnology, sc-16756) and monoclonal antibody against AIF (EPITOMICS, ab32516) diluted 1:100 in PBS-0.1% BSA, overnight at 4°C, washed 5 times with PBS, incubated with the secondary antibodies: anti-goat (Invitrogen, A11055, Alexa Fluor) and anti-rabbit (Invitrogen, A10040, Alexa Fluor) diluted 1:200 in PBS and incubated for 1 h at room temperature in a humidified chamber. Cells were then washed 3 times with PBS in the dark and finally mounted with Fluoromount (Sigma Life Sciences). For LEI/L-DNase II, cell labeling was performed as described before (Altairac *et al.*, 2003). For cleaved Caspase-3 labeling, after fixation and permeabilization performed as above, cells were washed 3 times with PBS and then saturated with 1% skim milk in PBS for 1 h. Cells were then incubated with monoclonal antibody against active Caspase-3 (Cell Signaling, 9661S) diluted 1:100 in 0.1% skim milk PBS, overnight at 4°C, washed 5 times for 5 min with PBS, incubated with the secondary antibody (Invitrogen, A10040, Alexa Fluor anti-rabbit) diluted 1:200 in PBS, for 1 h at room temperature in a humidified chamber. Cells were then washed 3 times with PBS in the dark and finally mounted with Fluoromount (Sigma Life Sciences). Cells were observed using a fluorescence microscope Olympus BX51, equipped with 40 × and 60 × objectives. Confocal analysis was performed using a Zeiss LMS710 microscope. Adobe Photoshop was used as the elaborating software.

Cytoplasm and Nucleus Fractions. Cells were collected by trypsinization and rinsed twice in PBS, then, 2×10^6 cells were resumed in 500 µl of a hypotonic solution of $MgCl_2$ (1.5mM) during 10 min. Cells were then crushed with a Dounce potter and centrifuged for 10 min at 390 × g. The cytoplasmic fraction contained in the supernatant was removed and the nuclear fraction was resuspended in 1 ml of $MgCl_2$ (1.5mM) and centrifuged for 10 min at 390 × g twice, then resuspended in 200 µl of 10mM Tris, 60mM NaCl, 200mM sucrose pH 7.4.

To measure the concentration of proteins in both cellular fractions, 10 µl of the cytoplasmic and nuclear fractions were mixed to 250 µl of reactive solution (Pierce BCA Protein Assay Kit, 23225) in a 96-multi-wells plate. The plate was incubated for 30 min at 37°C then the optical density was read in a BioRad Benchmark plate reader at 595 nm. The obtained measures were correlated to a standard curve of bovine serum albumin (BSA) made in duplicate (0–1200 µg/µl). The sample concentration was calculated by linear regression.

Western Blot Analysis

Cells were disrupted in RIPA buffer (50mM Tris, 150mM NaCl, 1% Triton-X100, 1% sodium deoxycholate, and 1% sodium dodecyl sulfate) or M-PER buffer (Thermo Scientific, 78503) in the presence of protease and phosphatase inhibitors. The protein concentration was determined by the BCA method (as previously described). The proteins were distorted in Laemmli (62mM Tris-HCl 6.8 pH, 2% SDS, 10% glycerol, 5% β-mercaptomethanol, and 0.01% bromophenol blue). Equal amounts of protein (20 µg) were separated on a 12% Tris-glycine gel. Nitrocellulose membrane transfer was performed at 100 V for 1:30 h at 4°C and monitored by the membrane staining with Ponceau Red (Sigma-Aldrich). The membrane was saturated with 5% skim milk in PBS for 1 h at room temperature then incubated overnight at 4°C with the primary antibodies against Caspase-3 (1:1000) (Santa

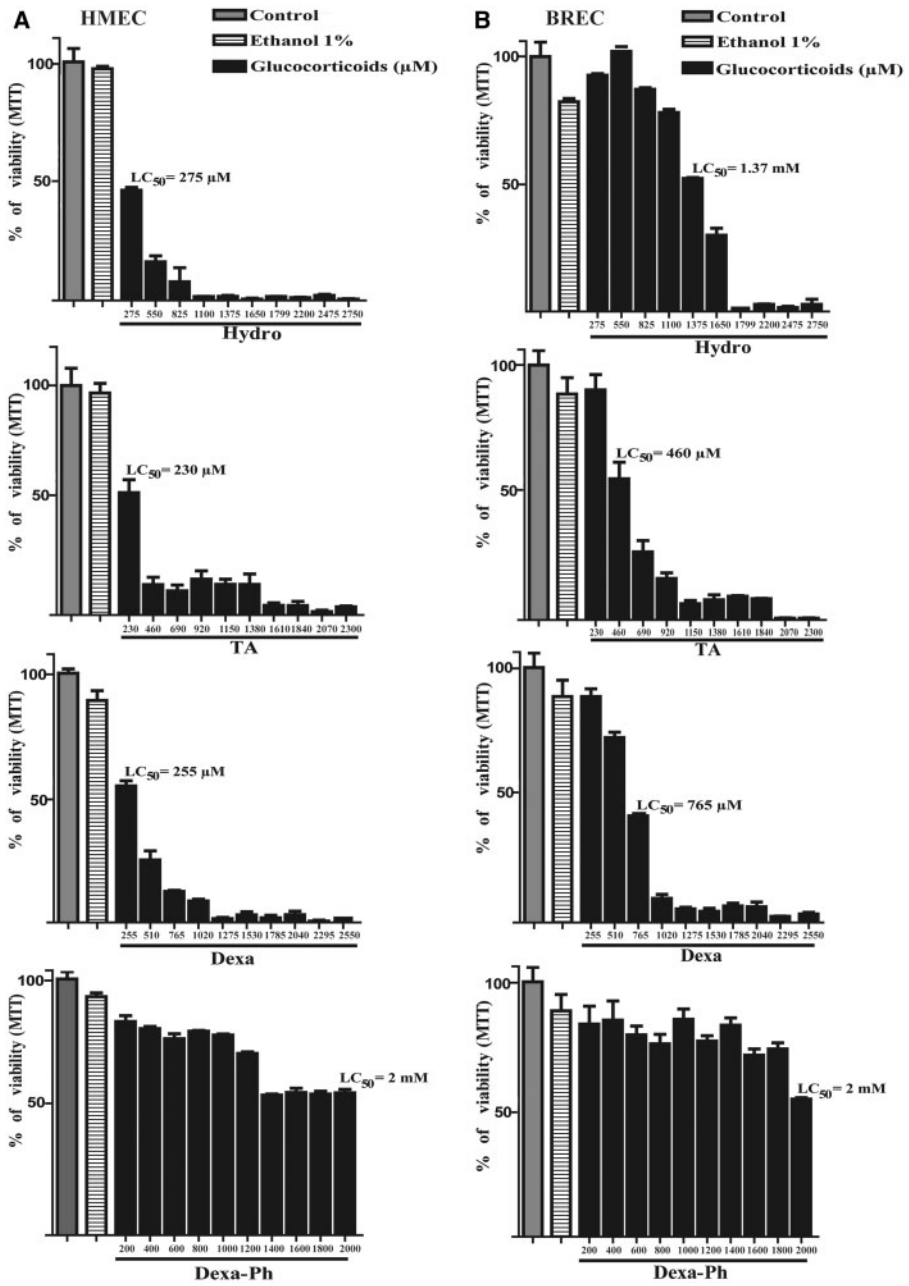

FIG. 1. Evaluation of the toxicity and lethal dose (LC_{50}) of different glucocorticoids (GCs) on human endothelial cells (HMECs) or bovine retinal endothelial cells (BRECs). Cells were treated with hydrocortisone (Hydro), triamcinolone acetonide (TA), dexamethasone (Dexa), dexamethasone-phosphate (Dexa-Ph) for 24 h at the indicated concentrations. The lipophilic GCs (Hydro, TA, and Dexa) were dissolved in ethanol 100% then in cell culture medium. Control cells were either exposed to 1% ethanol or were left untreated. Cell viability was evaluated using the MTT assay. A, HMEC; B, BREC. The lipophilic GCs show a concentration-response relationship between the decline of viability and the increase of the dose while Dexa-Ph is less toxic. These are representative results of 3 different experiments.

Cruz, 1224), cleaved Caspase-3 (1:1000) (Cell Signaling, 9661), AIF (1:1000) (Santa Cruz, 9416), LEI/L-DNase II (1:1000) (Torriglia *et al.*, 1995), β-actin (1:1000) (Santa Cruz, 1616), Lamin B (1:1000) (Santa Cruz, 6216), and LC3-II (1:1000) (Santa Cruz sc-16756). After 5 washes in PBS containing 0.1% Tween-20, the membrane was incubated for 1 h with the anti-rabbit (Victor Laboratories, PI-1000) or anti-goat (Victor Laboratories, PI-9500) secondary antibodies conjugated to peroxidase, diluted 1:5000, in PBS containing 0.5% skim milk and then washed 5 times in PBS. Poly ADP-ribose polymerase (PARP) Western blot was performed as already described by Blenn *et al.* (2006). Visualization of the immunoreactive bands was obtained by a chemoluminescent substrate, SuperSignal West Pico Chemiluminescent Substrate (Thermo scientific, 34087) using a MicroChemi 4.2 DNR BioImaging System.

Retinal Flat Mounting

After GCs treatment, retinas were immediately washed and fixed with 4% paraformaldehyde for 15 min. They were then permeabilized with PBS containing 0.1% Triton X-100, and incubated with the rabbit anti-Caspase-3 and mouse anti-von Willebrand antibody or the chicken anti-LEI, and rabbit anti-von

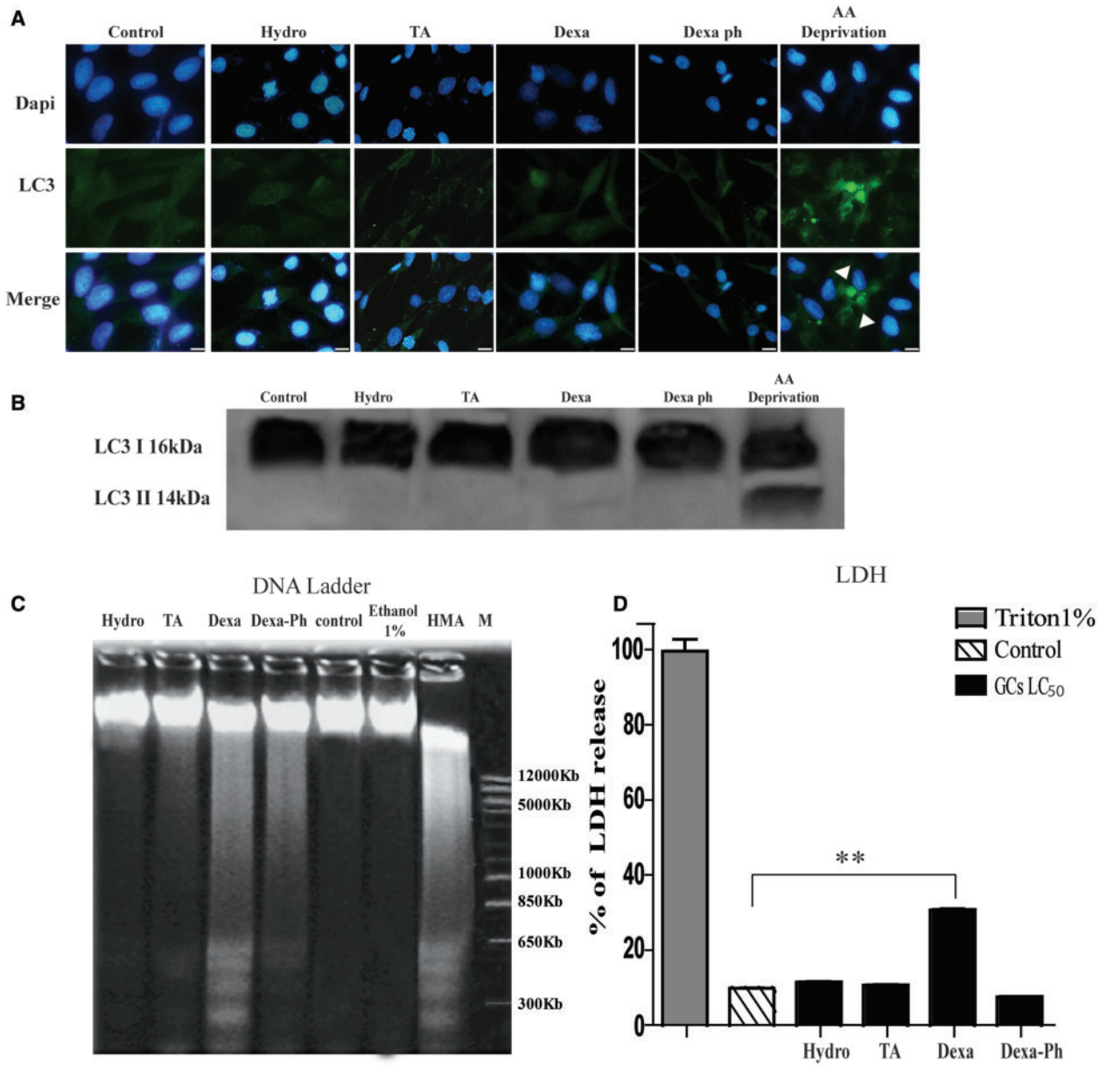

FIG. 2. Cell death in GCs treated HMEC cells. A, The activation of autophagy process was evaluated by anti-LC3 immunocytochemistry. HMECs were treated for 24 h with the LC_{50} of GCs. They were then fixed, permeabilized, and immunostained with anti-LC3 (green). For the positive control, cells were incubated with medium lacking amino acids (arrow heads). All treatments revealed diffuse cellular labeling of LC3 confirming the absence of autophagic vesicles. Scale bars represent 5 μm. B, Cells treated as above were analyzed by Western blot. The activation of autophagy in AA deprived cells triggers the appearance of a 14 kDa band, LC3II, the lipidated form of LC3. C, DNA extracted from HMEC treated with LC_{50} of GCs was analyzed by electrophoresis on a 2% agarose gel. Oligonucleosomal fragments of DNA are seen with Dexa, Dexa-Ph, and slightly with TA. Control: untreated cells, ethanol 1%: medium containing 1% of ethanol, treatment with 40 μm 5 -N, N-hexamethylene-amiloride (HMA) was used as a positive control for apoptosis. D, The release of lactate dehydrogenase (LDH) from HMECs treated 24 h with LC_{50} of GCs was measured in the culture medium and compared with the maximal LDH release, determined by exposing the cells to 1% of Triton X-100. Each experiment was performed in triplicate. Data are expressed as medium percentage of LDH released into the media. Dexa induced an increased release of LDH when compared with control and to the other treatments (**$P \leq 0.01$). This is a representative experiments out of 4.

Willebrand (1:100) overnight at 4°C. After washing 5 times with PBS, retinas were incubated with the secondary antibody (Alexa Fluor 405-conjugated goat anti-rabbit IgG and Alexa Fluor 594-conjugated Donkey anti-mouse IgG or Alexa Fluor 568-conjugated goat anti-chicken IgG, and Alexa Fluor 405-conjugated goat anti-rabbit IgG (1:200)) for 1 h. For phosphatase treatment, retinas were incubated for 30 min at 37°C with calf intestinal alkaline phosphatase (Invitrogen, 8009-019) in dephosphorylation buffer (Invitrogen, P/N 01371) then washed 3 times. Dephosphorylation was performed to unmask 3′-OH DNA extremity stemming from activation of L-DNase II. Finally, Retinas were fixed with 4% paraformaldehyde then incubated for 1 h with 80 μl of terminal deoxynucleotidyl transferase dUTP nick end labeling assay (TUNEL, Roche Diagnostics, Mannheim, Germany) reaction mixture at 37°C. The retinas were flat mounted using Fluoromount. Images were taken using a confocal laser scanning microscope Zeiss LSM 710 (Oberkochen, Germany).

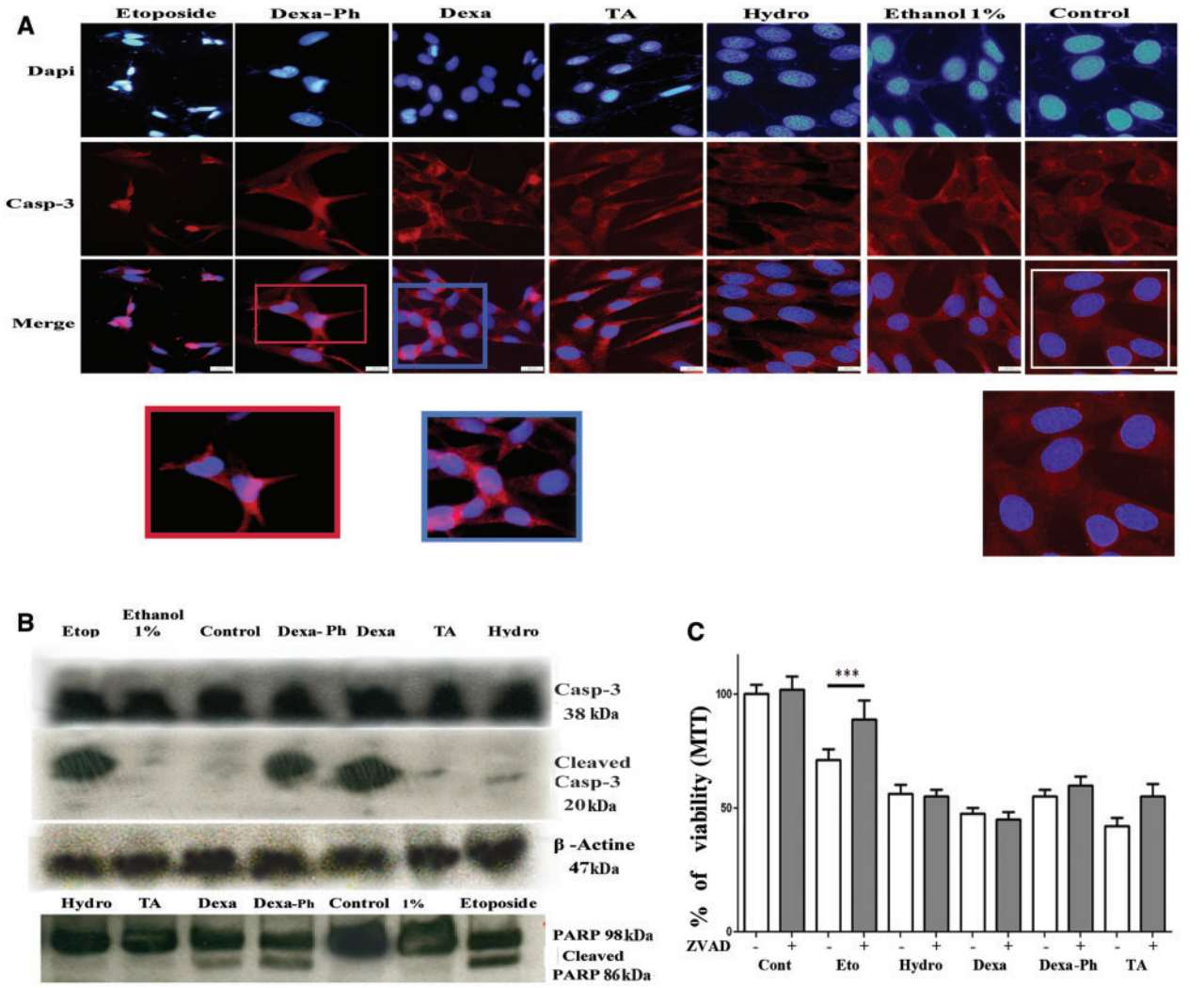

FIG. 3. The activation of caspases in GCs treated HMECs. A, The activation of Caspase-3 by immunolabeling of HMECs using an anti-active Caspase-3 antibody (red). Cells were exposed for 24 h with the LC_{50} of GCs. Cells incubated with etoposide were used as positive control. Only Dexa and Dexa-Ph induced an activation of Caspase-3 (higher magnifications below). These are representative results out of 3 independent experiments. Scale bars represent 7 μm. B, Caspase-3 and PARP Western blot analysis. Protein extracts from GCs-treated HMECs were analyzed in a 12% acrylamide gel, transferred to nitrocellulose and revealed with anti-Caspase-3. Apoptosis induced in HMECs with etoposide (100 μM for 24 h) was used as positive control. Activated Caspase-3 and cleaved PARP were detected in HMECs treated with Dexa and Dexa-Ph, showing that both GCs induce Caspase-3 activation. Representative results of 3 experiments. C, Effect of ZVAD on HMEC survival. Cells were exposed for 24 h with the LC_{50} of GCs in the presence (gray bars) or in the absence (white bars) of ZVAD-FMK. Cells incubated with Etoposide were used as positive control. MTT was used to evaluate cell viability. No protective effect is seen in GCs-treated cells. Results were analyzed by the ANOVA test using the Newman-Keuls post test. Asterisks (***) indicate significant differences $P < 0.001$.

Statistics

Data were expressed as means ± SE. Statistical analysis was performed using the Graphpad Prism5 program (Graphpad Software, San Diego, California). Mann-Whitney test comparison was used. $P < 0.05$ deemed significant, unless otherwise stated.

RESULTS

Dose-Dependent Effect of GCs on Microvascular Endothelial Cells Viability (HMEC, BREC) and Lethal Concentrations (LC_{50}) determination

In order to evaluate the sensitivity of HMEC and BREC to corticosteroids, cells were treated with different concentrations of Hydro, TA, Dexa, and Dexa-Ph for 24 h. Because hydrophobic GCs (Hydro, TA, and Dexa) form dense and adherent toxic aggregates when directly added to culture medium (Szurman *et al.*, 2007), they were first dissolved in ethanol 100%, then in the culture medium. This gave a final concentration of 1% ethanol in the medium. The reduced viability measured by the MTT assay was correlated to a reduced number of living cells, as verified by the trypan blue assay (not shown). Figure 1 shows that GCs had different concentrations-dependent reduction of cell viability, depending on the GC and the cell type. Dexa-Ph was the least toxic and HMECs were more sensitive than BRECs.

The Mechanisms of Cell Death Induced by GCs

In order to analyze the mechanisms underlying GC toxicity on endothelial cells, we successively evaluated markers for autophagy, necrosis, caspases-dependent and caspases-independent apoptosis. These analyses were performed on HMEC

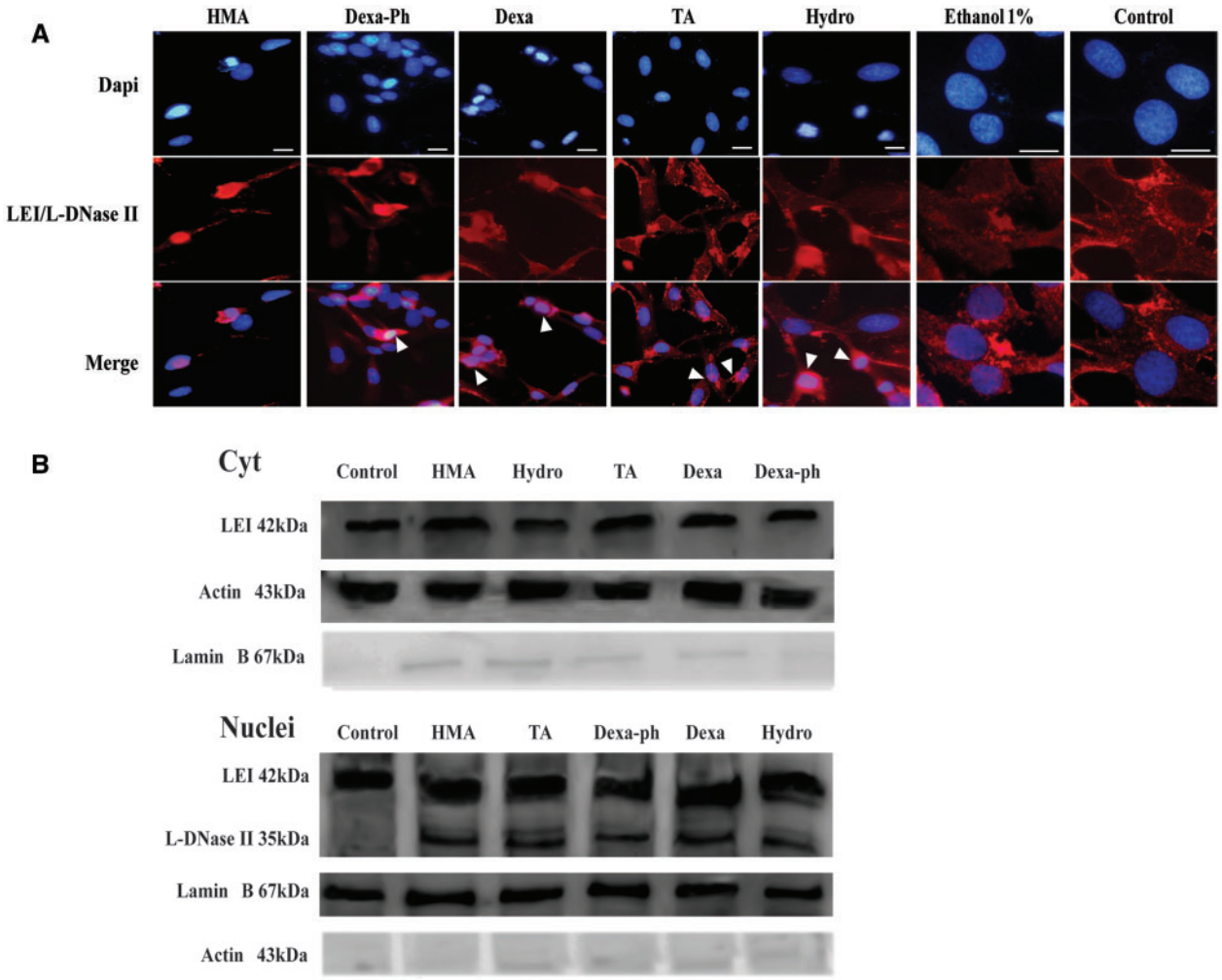

FIG. 4. Activation of the L-DNase II pathway in GCs-treated HMECs. A, HMEC cells were treated with the LC_{50} of GCs for 24 h and immunostained with an anti-LEI/L-DNase II (red). HMECs exposed to HMA represent the positive control. All the GCs led to LEI/L-DNase II activation with an intense nuclear staining (arrow heads). Scale bar represents 10 μm. These are representative results out of 4 experiments. B, GCs-treated HMECs were fractionated into cytoplasmic and nuclear fractions. Western blot analysis using an anti-LEI/L-DNase II revealed an accumulation of L-DNase II in the nucleus of treated cells, phenomena also seen in HMA-treated cells used as positive control.

using for each steroid the LC_{50} as determined above in order to have the same degree of toxicity.

Autophagy

The presence of autophagy was analyzed using an antibody against MAP-LC3 (*microtubule-associated protein 1 light chain 3*). This protein is integrated into the autophagosomes membranes (Tanida *et al.*, 2004). Under physiological conditions, the quiescent LC3 has a diffuse distribution in the cytoplasm. Once the autophagy is activated, LC3 concentrates in the autophagosome membrane and gives a punctuate labeling as observed in cells cultured in a depleted amino-acid (AA) medium, used as a positive control (Fig. 2A). No such labeling was observed with GCs treatment eliminating autophagy as a potential mechanism of cell death (Fig. 2A). This result was confirmed by Western blot. As seen in Fig. 2B, lipidated form of LC3 (LC3 II) only appeared in the AA depleted medium.

DNA Damage and Necrosis

DNA fragmentation into oligonucleosomal fragments is a well-recognized hallmark of apoptotic cell death, as induced by 5-N, N-hexamethylene-amiloride (HMA) (used as a positive control). The "DNA ladder" pattern was clearly seen in samples treated with Dexa and Dexa-Ph, faintly with TA treatment and not at all in Hydro-treated cells (Fig. 2C). Moreover, since a degree of smear degradation was observed, we investigated whether necrosis was involved by measuring the release of LDH in the culture medium. A total lysis of the cells induced by 1% Triton-X100 was used as a positive control. Among the GCs tested at their respective LC_{50} concentrations, only Dexa (255 μM) induced a significant increase of LDH release (31.17%; $^{**}P \leq 0.01$) when compared with the positive control (Fig. 2D).

Caspases-Dependent Apoptosis in GCs Toxicity

Caspase-3 activation was analyzed by immunocytochemistry (Fig. 3A) and Western blot (Fig. 3B). Among the GCs tested at their respective LC_{50} concentrations, only Dexa and Dexa-Ph induced activation of Caspase-3 as observed on immunocytochemistry (Fig. 3A). This was confirmed by Western blot (Fig. 3B). Only Dexa and Dexa-Ph induced the cleavage of pro-Caspase-3. Moreover, PARP-1, one of the main targets of

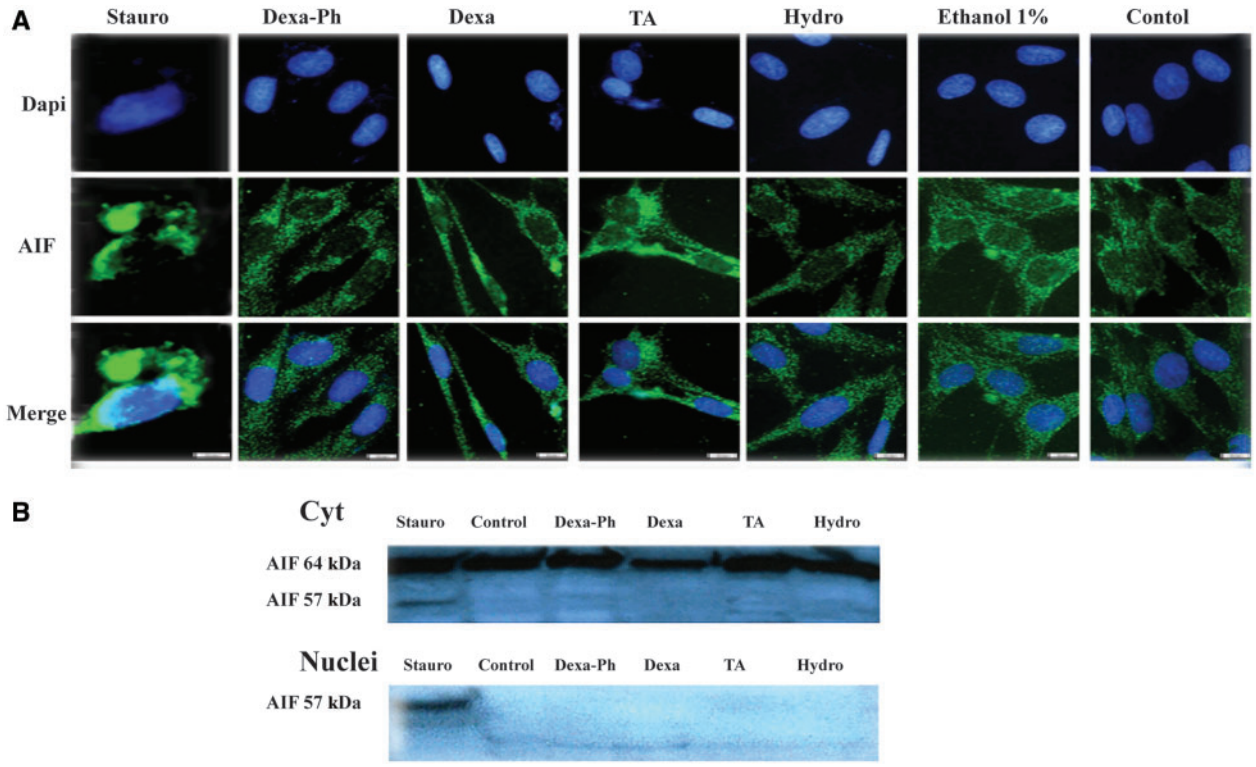

FIG. 5. AIF activation in GCs-treated HMECs. A, Nuclear translocation of AIF was evaluated by anti-AIF immunocytochemistry (green). HMECs were treated for 24 h with the LC_{50} of GCs, for the positive control cells were treated with Staurosporine (Stauro). Control cells and GCs-treated cells revealed a dotted labeling of AIF. Scale bars represent 10 μm. These are representative images of 2 independent experiments performed in quadruplicate. B, AIF Western blot was performed on nuclear and cytoplasmic fractions. AIF was present in all cytoplasmic fractions, only the Staurosporine-treated cells, used as a positive control, show a nuclear translocation of the truncated (active) form of AIF. Representative experiments out of 2.

activated Caspase-3 was cleaved in cells treated with Dexa and Dexa-Ph but not in cells treated with other GCs (Fig. 3B). In all these experiments, the treatment of cells with etoposide, an inhibitor of topoisomerase II, known to induce caspases-dependent cell death was used as a positive control. The involvement of caspases in cell death was evaluated using the pancaspase inhibitor ZVAD-FMK. Results are seen in Figure 3C. The inhibitor successfully inhibits cell death in etoposide but not in GCs-treated cells, suggesting that this pathway is not the main effector in GCs cell demise.

Caspases-Independent Apoptosis in GCs Toxicity

Due to the lack of caspases activation in TA and Hydro, as well as the lack of protection with pancaspase inhibitor, we analyzed caspases-independent pathways, namely LEI (LEI/L-DNase II) and AIF.

LEI is a cytoplasmic molecule owning an anti-protease activity. After induction of apoptosis it is cleaved and transformed into L-DNase II, a molecule that has an endonuclease activity and that is translocated to the nucleus (Padron-Barthe *et al.*, 2007).

The activation of L-DNase II was estimated by immunostaining and Western blot. L-DNase II activation and nuclear translocation were observed with all GCs (Fig. 4A). In order to verify the nuclear translocation of this protein, we fractionated the cytoplasm from nucleus, and performed a Western blot on both fractions (Fig. 4B). We observed the presence of native LEI (42 kDa) in the cytoplasmic fractions while the nuclear fractions contained, in addition, one band of 35 kDa corresponding to the active L-DNase II (Belmokhtar *et al.*, 2000). Taken together these results indicate that GCs activate the LEI/L-DNase II pathway. HMA-treated cells were used as positive control of L-DNase II activation.

Concerning AIF (Fig. 5), HMECs treated with the GCs presented a cytoplasmic dotted labeling that was compatible with its classical mitochondrial localization. This localization was not seen to be modified by the GCs (Fig. 5A). Observe that staurosporine-treated cells used as positive control of AIF activation showed a diffuse cytoplasmic labeling and a nuclear peripheral labeling. As previously done, we verified this result by Western blot (Fig. 5B) after nuclear-cytoplasmic fractionation. The activated, cleaved form of AIF is only seen in staurosporine-treated cells. These results indicate that the AIF is not activated by GCs in HMECs.

Effect of GCs on BREC

To verify whether the cellular phenomena induced by the GCs on the HMEC were reproducible on retinal endothelial cells, we analyzed the activation of the cell death pathways previously studied.

For this purpose, BRECs were treated for 24 h with LC_{50} then the activation of Caspase-3, LEI/L-DNase II, and AIF were estimated by immunostaining with the corresponding antibody. The activation of Caspase-3 was observed on BREC treated with Dexa and Dexa-Ph, as already indicated for HMEC. Hydro and TA did not induce the Caspase-dependent cell death (Fig. 6C). Similarly, the activation of the LEI and nuclear translocation of L-DNase II were observed with all GCs on BREC (shown in higher magnifications) (Fig. 6A). The analysis of the immunocytochemistry of AIF on BREC showed a cytoplasmic dotted labeling

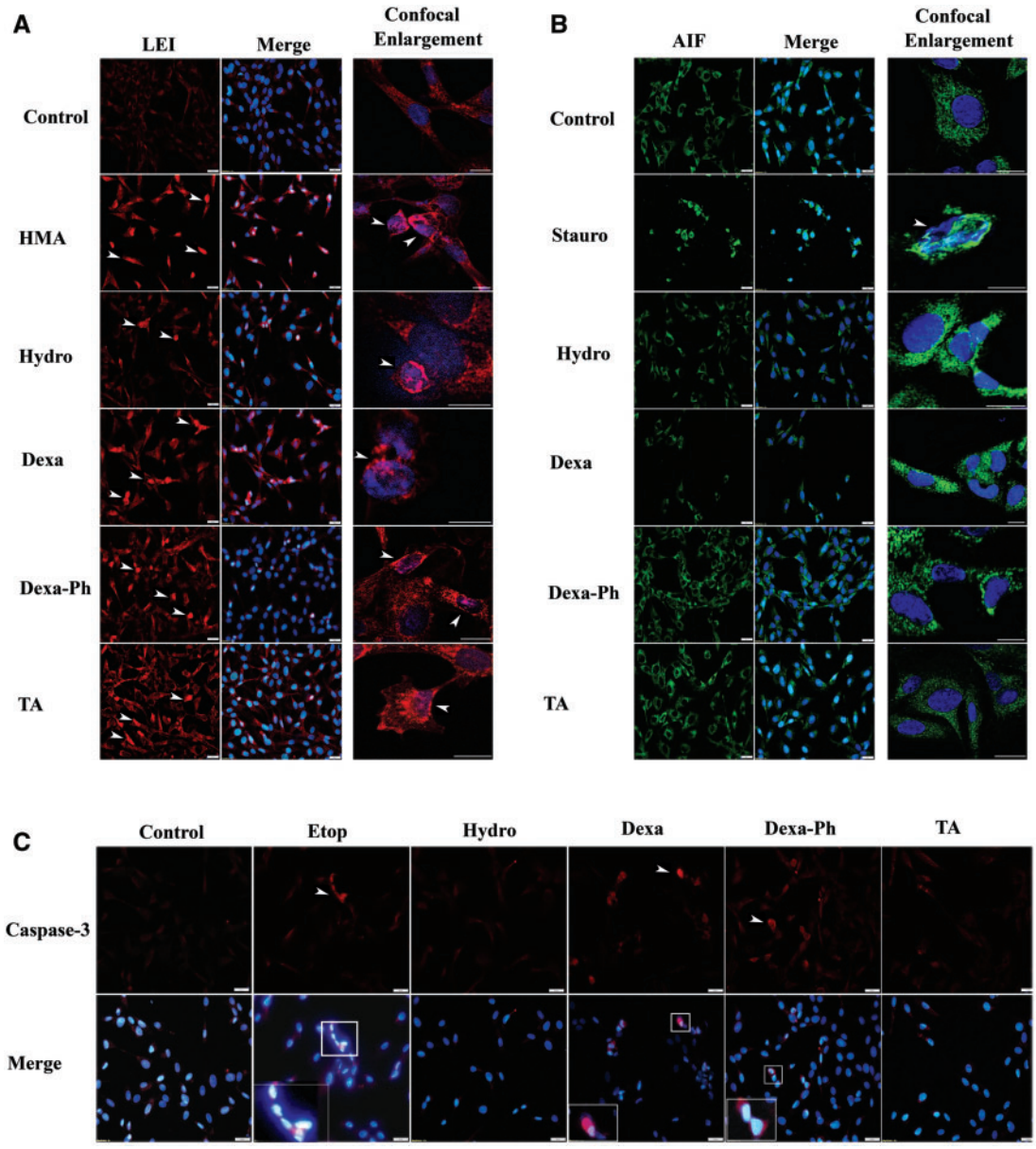

FIG. 6. The activation of caspases-dependent and independent cell death in GCs-treated BRECs. For all experiments, BREC were treated during 24 h with LC_{50} of GCs. A, BRECs were immunostained with an anti-LEI/L-DNase II. Cells exposed to HMA represent the positive control. All the GCs led to LEI/L-DNase II activation with an intense nuclear staining (white arrow heads) the same outcomes was observed previously with HMEC. LEI/L-DNase II was stained in red, nuclei in blue. The right column represents confocal images of cells showing a nuclear translocation of L-DNase II. Scale bars represent 20 μm for fluorescence images and 10 μm for confocal images. B, Nuclear translocation of AIF in BREC was evaluated by anti-AIF immunocytochemistry. Cells treated with Staurosporine represent a positive control. GCs-treated cells revealed a dotted labeling of AIF, which suggests a mitochondrial localization. White arrow head shows a nuclear translocation of AIF. AIF is seen in green, nuclei in blue. Scale bars represent 20 μm for fluorescence images and 10 μm for confocal images. C, Activated Caspase-3 immunocytochemistry of BRECs. BRECs were immunostained with an antibody that specifically recognizes the cleaved Caspase-3. Etoposide was used as a positive control. Like previously observed with HMECs only Dexa and Dexa-Ph induced an activation of Caspase-3 (arrow heads and magnifications). Activated Caspase-3 is seen in red, nuclei in blue. Scale bars represent 20 μm. All experiments were performed at least 4 times.

indicating the mitochondrial localization of AIF with all GCs treatments, while cells treated with the staurosporine (positive control) revealed a diffuse labeling in the cytoplasm and a nuclear translocation (Fig. 6B).

Impact of GCs on the Retinal Microvasculature

The *in vitro* experiments described above demonstrated the toxic effects of GCs on HMEC and BREC. In order to mimic physiological conditions more closely, where the endothelial cells are organized as microvascular networks, rat retina explants were treated with GCs for 24 h at the LC_{50} determined for BREC cells. An "*ex vivo*" model was preferred to an "*in vivo*" approach in order to better control the concentration of GCs reaching the retinal vascular bed. During intravitreal administration of drugs in rodents, due to the relatively large lens, there is a non-homogeneous distribution of the injected substance and an uneven concentration reaching different parts of the retina. The retinal microvasculature was immunostained with anti-Von

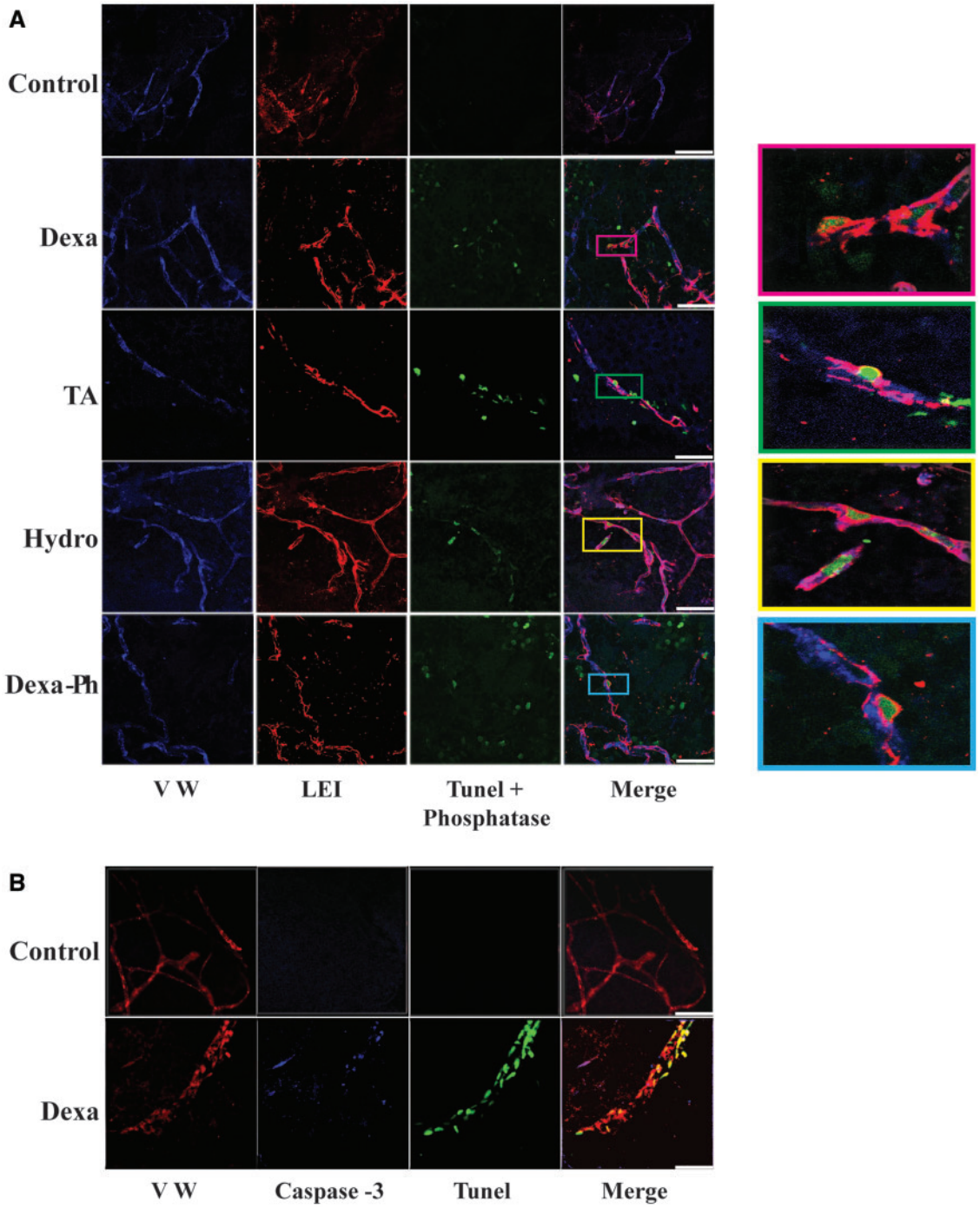

FIG. 7. Cell death pathway induced by GCs on retinal microvasculature. Retinas from Lewis rats were flat mounted, treated with GCs, and analyzed. The retinas treated with steroids-free medium were used as control. A, Retinal explants were treated with GCs, and immunostained for LEI/L-DNase II (red), TUNEL-phosphatase (green), and won Willebrand factor (blue). L-DNase II was activated with all treatments. Magnifications of cells displaying L-DNase II activation are seen on the right. B, Retinal explants were treated with GCs, and immunostained for Caspase-3 (blue), TUNEL (green), and won Willebrand factor (red). The activation of Caspase-3 on retina vessels was induced with Dexa. Scale bar represents 30 μm. Each experiment was performed at least 4 times.

Willebrand antibody. The double immunolabeling anti-caspase with TUNEL assay or anti-LEI/L-DNase II with TUNEL + phosphatase assay allowed us to analyze the activation of these cell death pathways. As for HMEC and BREC, LEI/L-DNase II was activated on retina microvascular cells with all tested GCs as observed in our *in vitro* experiments (Fig. 7A). The activation of Caspase-3 was observed in Dexa and Dexa-Ph treatments, whereas Hydro and TA did not induce a caspases-dependent cell death (Fig. 7B).

DISCUSSION

Intraocular GCs are widely used to treat retinal diseases, directly injected into the vitreous as a non-soluble crystal suspension

(such as TA) or more recently as polymeric poly-lactic-co-glycolic acid implants releasing Dexa. The choice of the GC is empirical since very few studies have compared their potential toxic and beneficial effects. In this study, we investigate the potential toxicity of GCs on the microvasculature. We have focused on the established microvasculature rather than neovascularization which has already been featured in previous studies. Cellular models have limitations and extrapolation to clinical conditions or to established tissues should be performed with caution. In our experiments, we use confluent cells, so that our experimental conditions are closer to established vessels than to proliferating vessels. In our retinal explants, we evaluate resting vessels rather than proliferating vessels. We compare two cell lines of dermal and retinal origin in order to investigate the differences in toxicity and we further evaluated the underlying mechanisms of different GCs toxicity. Our results show that endothelial cells originating from the retina (BREC) are less sensitive to all the GCs tested when compared with endothelial cells from dermal origin (HMEC). Although the cells are from different origins in terms of species and the cells have different culture conditions, various factors concerning the tissue origin of the cells could explain the difference in GCs sensitivity. The first factor could be the natural microenvironment of these cells. In the eye, cortisol levels are higher than in the circulation and the corticoid-binding globulin is absent, explaining in part the immunologic privilege of the intraocular media (Denniston *et al.*, 2011). Moreover, in inflammatory conditions, as shown in experimental models of uveitis, cortisol levels increase in the ocular media (Bousquet *et al.*, 2012). This permanent exposure to high cortisol levels associated with the low proliferating capacity of retinal endothelial cells may explain their higher resistance to GCs-induced cell death (Joussen *et al.* 2007).

Although the tested drugs belong to the same pharmacological family, they show different cellular toxicity. One might think that these different effects could be related to their relative affinity for glucocorticoid or mineralocorticoid receptors (Chen *et al.*, 2002). However, the concentrations of GCs used here are greater than the binding constant of these receptors (in the micromolar range), the receptors are completely saturated, suggesting that the toxic effects are receptor independent.

Concerning endothelial cell toxicity, our results show that hydrophilic GC, Dexa-Ph is less toxic than the lipophilic, Hydro, Dexa, and TA. This difference may be explained, by hydrophilic GCs transferring less easily through the intact membranes, resulting in lower bioavailability in cells and less toxicity. It is worth noting that the toxicity measured here is not related to the anti-inflammatory activity of these compounds. Compared with Hydro, TA has 5- to10-fold greater anti-inflammatory activity, whereas Dexa has 20- to 40-fold greater activity. However, their LC_{50} values are quite similar (255μM for Dexa and 230μM for TA) (Cohen and Jacquot, 1981; Le Jeunne, 2012).

TA is the most widely administered intraocular GC and is usually given in a formulation not specifically adapted to ophthalmological use, as it was originally designed for intramuscular and intra-articular administration. Studies on the toxicity of TA and/or its excipient (benzylic alcohol), the crystalline or soluble formulations, have led to conflicting rather than concluding results (Torriglia *et al.*, 2010, Valamanesh *et al.*, 2007). Indeed, toxicity of TA and its excipient was not found in certain studies (McCuen, 1981; Narayanan *et al.*, 2006) while other works clearly established the toxicity of TA and/or the excipient in the eye, resulting in a disorganization of the retina layers, a loss of the choroid network density and a vasoconstriction of the retina blood vessels (Morrison *et al.*, 2006; Torriglia *et al.*, 2010; Valamanesh *et al.*, 2009).

TA showed concentration and time-dependent cytotoxicity on retinal pigment epithelium cells, glial cells, and endothelial cells of the retina. This toxicity triggered a reduction in mitochondrial activity, and an activation of caspases-independent cell death mechanism (paraptosis in EPR cells, LEI-L-DNase II, and AIF in retinal endothelial cells [Narayanan *et al.*, 2006; Valamaneshet *al.*, 2007; Yeung *et al.*, 2003]). This may explain the results obtained by some authors that showed no caspase activation after 24 h of treatment with TA on primary human retinal microvascular and flat mounted rat retinas (Hartnett *et al.*, 2006). Hence, the assessment of cell death pathways is an essential step in estimating the safety or the toxicity of health products. We show that different cell death mechanisms other than classical caspases-dependent apoptosis may be responsible for cell death induced by GCs and that the same mechanisms seen in cell culture were also seen ex-*vivo* (retinal microvessels). Moreover, the use of the pancaspase inhibitor, ZVAD on HMEC does not reveal a protective activity with any of the GCs suggesting that caspases are not the main effectors in this cell death.

In this study, the toxicity of several GCs is estimated and compared for the first time, on microvascular endothelial cells of different tissue origins. GCs toxicity was previously disregarded because the tests used were unsuitable for evaluating caspases-independent cell death. Strikingly, the concentrations used in our experiments, which proved to be cytotoxic, were lower than those used clinically. For instance, 4 mg of TA is usually injected into the human vitreous to treat macular edema. This produces a concentration of 1 mg/ml (approximately 2.3mM) of TA in the vitreous (lasting up to 1 month) due to the slow clearance of drugs in this compartment. The vitreous humor levels measured by several authors after TA intravitreous injection, are higher than the LC_{50} found in both HMEC and BREC (around 4mM when compared with 230 μM and 460μM for HMEC and BREC, respectively) (Oliveira *et al.*, 2012).

GCs have widespread clinical applications in the eye and in other organs and their use is often the only available therapeutic option. In this work, we demonstrate that at high concentrations these compounds may be toxic to endothelial cells of the microvasculature and other target tissues. It is essential to ensure that these concentrations remain under the toxic threshold for endothelial cells when developing novel therapeutic protocols.

FUNDING

This work was funded by the Institut National de la santé et de la recherche médicale (INSERM).

ACKNOWLEDGMENTS

The authors acknowledge Dr Gloria Villalpando Rodriguez and Dr Eamon Sharkawi for their help with the English version of the article. Nothing to disclose.

REFERENCES

Ades, E. W., Candal, F. J., Swerlick, R. A., George, V. G., Summers, S., Bosse, D. C., and Lawley, T. J. (1992). Hmec-1: establishment of an immortalized human microvascular endothelial cell line. *J. Invest. Dermatol.* **99,** 683–690.

Allen, D. B., Bielory, L., Derendorf, H., Dluhy, R., Colice, G. L., and Szefler, S. J. (2003). Inhaled corticosteroids: past lessons and future issues. *J. Allergy Clin. Immunol.* **112,** S1–S40.

Altairac, S., Zeggai, S., Perani, P., Courtois, Y., and Torriglia, A. (2003). Apoptosis induced by Na+/H+ antiport inhibition

activates the LEI/L-DNase II Pathway. *Cell Death Differ*. **10,** 548–557.

Anacker, C., Zunszain, P. A., Carvalho, L. A., and Pariante, C. M. (2011). The glucocorticoid receptor: pivot of depression and of antidepressant treatment? *Psychoneuroendocrinology* **36,** 415–425.

Barnes, P. J. (2005). Molecular mechanisms and cellular effects of glucocorticosteroids. *Immunol. Allergy Clin. North Am.* **25,** 451–468.

Behar-Cohen, F. (2011). [Retinal drug targets]. *Ann. Pharm. Fr.* **69,** 124–130.

Belmokhtar, C. A., Torriglia, A., Counis, M. F., Courtois, Y., Jacquemin-Sablon, A., and Segal-Bendirdjian, E. (2000). Nuclear translocation of a leukocyte elastase inhibitor/elastase complex during staurosporine-induced apoptosis: role in the generation of nuclear L-DNase II activity. *Exp. Cell Res.* **254,** 99–109.

Blenn, C., Althaus, F. R., and Malanga, M. (2006). Poly(Adp-ribose) glycohydrolase silencing protects against H_2O_2-induced cell death. *Biochem. J.* **396,** 419–429.

Bousquet, E., Zhao, M., Ly, A., Leroux Les Jardins, G., Goldenberg, B., Naud, M. C., Jonet, L., Besson-Lescure, B., Jaisser, F., Farman, N., *et al.* (2012). The aldosterone-mineralocorticoid receptor pathway exerts anti-inflammatory effects in endotoxin-induced uveitis. *PLoS One* **7,** e49036.

Capetandes, A., and Gerritsen, M. E. (1990). Simplified methods for consistent and selective culture of bovine retinal endothelial cells and pericytes. *Invest. Ophthalmol. Vis. Sci.* **31,** 1738–1744.

Chan, C. K., Ip, M. S., Vanveldhuisen, P. C., Oden, N. L., Scott, I. U., Tolentino, M. J., and Blodi, B. A. (2011), Score study report #11: incidences of neovascular events in eyes with retinal vein occlusion. *Ophthalmology* **118,** 1364–1372.

Chen, W., Lee, J. Y., and Hsieh, W. C. (2002). Effects of dexamethasone and sex hormones on cytokine-induced cellular adhesion molecule expression in human endothelial cells. *Eur. J. Dermatol.* **12,** 445–448.

Cockrem, J. (2013). Individual variation in glucocorticoid stress responses in animals. *Gen. Comp. Endocrinol.* **181,** 45–58.

Cohen, Y., and Jacquot, C. (1981). *Pharmacologie. Médicaments Anti-Inflammatoires*. Elservier Masson 2008 ed. Paris. p. 334.

Denniston, A. K., Kottoor, S. H., Khan, I., Oswal, K., Williams, G. P., Abbott, J., Wallace, G. R., Salmon, M., Rauz, S., Murray, P. I., *et al.* (2011). Endogenous cortisol and Tgf-beta in human aqueous humor contribute to ocular immune privilege by regulating dendritic cell function. *J. Immunol.* **186,** 305–311.

Folkman, J., and Ingber, D. E. (1987). Angiostatic steroids. Method of discovery and mechanism of action. *Ann. Surg.* **206,** 374–383.

Folkman, J., Langer, R., Linhardt, R. J., Haudenschild, C., and Taylor, S. (1983). Angiogenesis inhibition and tumor regression caused by heparin or a heparin fragment in the presence of cortisone. *Science* **221,** 719–725.

Galluzzi, L., Vitale, I., Abrams, J. M., Alnemri, E. S., Baehrecke, E. H., Blagosklonny, M. V., Dawson, T. M., Dawson, V. L., El-Deiry, W. S., Fulda, S., *et al.* (2012). Molecular definitions of cell death subroutines: recommendations of the nomenclature committee on cell death 2012. *Cell Death Differ.* **19,** 107–120.

Geltzer, A., Turalba, A., and Vedula, S. S. (2013). Surgical implantation of steroids with antiangiogenic characteristics for treating neovascular age-related macular degeneration. *Cochrane Database Syst. Rev.* **1,** CD005022.

Hartnett, M. E., Martiniuk, D. J., Saito, Y., Geisen, P., Peterson, L. J., and McColm, J. R. (2006). Triamcinolone reduces neovascularization, capillary density and Igf-1 receptor phosphorylation in a model of oxygen-induced retinopathy. *Invest. Ophthalmol. Vis. Sci.* **47,** 4975–4982.

Hu, Z. M., Wang, H. B., Zhou, M. Q., Yao, X. S., Ma, L., and Wang, X. N. (2006). [Pathological changes of the blood vessels in rabbit femoral head with glucocorticoid-induced necrosis]. *Nan Fang Yi Ke Da Xue Xue Bao* **26,** 785–787.

Joussen, A., Gardner, T., Kirchhof, B., and Ryanpage, S. (2007). *Retinal Vascular Disease*. Springer-Verlag. Berlin Heildelberg, NY, pp. 3–6.

Katychev, A., Wang, X., Duffy, A., and Dore-Duffy, P. (2003). Glucocorticoid-induced apoptosis in CNS microvascular pericytes. *Dev. Neurosci.* **25,** 436–446.

Knisely, T. L., Hosoi, J., Nazareno, R., and Granstein, R. D. (1994). The presence of biologically significant concentrations of glucocorticoids but little or no cortisol binding globulin within aqueous humor: relevance to immune privilege in the anterior chamber of the eye. *Invest. Ophthalmol. Vis. Sci.* **35,** 3711–3723.

Le Jeunne, C. (2012). Pharmacologie Des Glucocorticoïdes. *La Presse Médicale* **41,** 370–377.

Logie, J. J., Sadaf, A., Marshall, M., Margarete, M., Heck, B. R., Walker, P., and Hadoke, F. (2010). Glucocorticoid-mediated inhibition of angiogenic changes in human endothelial cells is not caused by reductions in cell proliferation or migration. *PLoS One* **5,** e14476.

McCuen B. W., II, Bessler M., Tano, Y., Chandler, D., and Machemer, R. (1981). The lack of toxicity of intravitreally administered triamcinolone acetonide. *Am. J. Ophthalmol.* **91,** 785–788.

Miyamoto, N., Iossifov, D., Metge, F., and Behar-Cohen, F. (2006). Early effects of intravitreal triamcinolone on macular edema: mechanistic implication. *Ophthalmology* **113,** 2048–2053.

Morrison, V. L., Koh, H. J., Cheng, L., Bessho, K., Davidson, M. C., and Freeman, W. R. (2006). Intravitreal toxicity of the kenalog vehicle (benzyl alcohol) in rabbits. *Retina* **26,** 339–344.

Mosmann, T. (1983). Rapid colorimetric assay for cellular growth and survival: application to proliferation and cytotoxicity assays. *J. Immunol. Methods* **65,** 55–63.

Narayanan, R., Mungcal, J. K., Kenney, M. C., Seigel, G. M., and Kuppermann, B. D. (2006). Toxicity of triamcinolone acetonide on retinal neurosensory and pigment epithelial cells. *Invest. Ophthalmol. Vis. Sci.* **47,** 722–728.

Ning Zhua, Z. W. (1997). An assay for DNA fragmentation in apoptosis without phenol/chloroform extraction and ethanol precipitation. *Anal. Biochem.* **246,** 155–158.

Oliveira, R. C., Messias, A., Siqueira, R. C., Bonini-Filho, M. A., Haddad, A., Damico, F. M., Maia-Filho, A., Crispim, P. T., Saliba, J. B., Ribeiro, J. A., *et al.* (2012). Vitreous pharmacokinetics and retinal safety of intravitreal preserved versus non-preserved triamcinolone acetonide in rabbit eyes. *Curr. Eye Res.* **37,** 55–61.

Padron-Barthe, L., Lepretre, C., Martin, E., Counis, M. F., and Torriglia, A. (2007). Conformational modification of serpins transforms leukocyte elastase inhibitor into an endonuclease involved in apoptosis. *Mol. Cell Biol.* **27,** 4028–4036.

Schacke, H., Docke, W. D., and Asadullah, K. (2002). Mechanisms involved in the side effects of glucocorticoids. *Pharmacol. Ther.* **96,** 23–43.

Sharma, A., Pirouzmanesh, A., Patil, J., Estrago-Franco, M. F., Zacharias, L. C., Andley, U. P., Kenney, M. C., and Kuppermann, B. D. (2011). Evaluation of the toxicity of

triamcinolone acetonide and dexamethasone sodium phosphate on human lens epithelial cells (Hle B-3). *J. Ocul. Pharmacol. Ther.* **27,** 265–271.

Shikatani, E. A., Trifonova, A., Mandel, E. R., Liu, S. T., Roudier, E., Krylova, A., Szigiato, A., Beaudry, J., Riddell, M. C., and Haas, T. L. (2012). Inhibition of proliferation, migration and proteolysis contribute to corticosterone-mediated inhibition of angiogenesis. *PLoS One* **7,** e46625.

Small, G. R., Hadoke, P. W., Sharif, I., Dover, A. R., Armour, D., Kenyon, C. J., Gray, G. A., and Walker, B. R. (2005). Preventing local regeneration of glucocorticoids by 11beta-hydroxysteroid dehydrogenase type 1 enhances angiogenesis. *Proc. Natl Acad. Sci. U. S. A.* **102,** 12165–12170.

Schmidt, M., Pauels, H. G., Lugering, N., Lugering, A., Domschke, W., and Kucharzik, T. (1999). Glucocorticoids induce apoptosis in human monocytes: potential role of IL-1 beta. *J Immunol* **163,** 3484–90.

Szurman, P., Sierra, A., Kaczmarek, R., Jaissle, G. B., Wallenfels-Thilo, B., Grisanti, S., Luke, M., Bartz-Schmidt, K. U., and Spitzer, M. S. (2007). Different biocompatibility of crystalline triamcinolone deposits on retinal cells in vitro and in vivo. *Exp. Eye Res.* **85,** 44–53.

Tanida, I., Ueno, T., and Kominami, E. (2004). Lc3 conjugation system in mammalian autophagy. *Int. J. Biochem. Cell Biol.* **36,** 2503–2518.

Torriglia, A., Chaudun, E., Chany-Fournier, F., Jeanny, J. C., Courtois, Y., and Counis, M. F. (1995). Involvement of DNase II in nuclear degeneration during lens cell differentiation. *J. Biol. Chem.* **270,** 28579–28585.

Torriglia, A., Valamanesh, F., and Behar-Cohen, F. (2010). On the retinal toxicity of intraocular glucocorticoids. *Biochem. Pharmacol.* **80,** 1878–1886.

Valamanesh, F., Berdugo, M., Sennlaub, F., Savoldelli, M., Goumeaux, C., Houssier, M., Jeanny, J. C., Torriglia, A., and Behar-Cohen, F. (2009). Effects of triamcinolone acetonide on vessels of the posterior segment of the eye. *Mol. Vis.* **15,** 2634–2648.

Valamanesh, F., Torriglia, A., Savoldelli, M., Gandolphe, C., Jeanny, J. C., BenEzra, D., and Behar-Cohen, F. (2007). Glucocorticoids induce retinal toxicity through mechanisms mainly associated with paraptosis. *Mol. Vis.* **13,** 1746–1757.

Walker, J. J., Spiga, F., Waite, E., Zhao, Z., Kershaw, Y., Terry, J. R., and Lightman, S. L. (2012). The origin of glucocorticoid hormone oscillations. *PLoS Biol.* **10,** e1001341.

Yeung, C. K., Chan, K. P., Chiang, S. W., Pang, C. P., and Lam, D. S. (2003). The toxic and stress responses of cultured human retinal pigment epithelium (Arpe19) and human glial cells (Svg) in the presence of triamcinolone. *Invest. Ophthalmol. Vis. Sci.* **44,** 5293–5300.